Reduction of self-phase-modulation induced phase jitter in multiplexing repetition rate of actively mode-locked laser for photonic analog-to-digital converters

Conference Paper *in* Proceedings of SPIE - The International Society for Optical Engineering · February 2015

DOI: 10.1117/12.2077925

CITATIONS
0

READS
31

3 authors:

Si Chen
Shanghai Jiao Tong University
3 PUBLICATIONS **0** CITATIONS
SEE PROFILE

Guang Yang
Shanghai Jiao Tong University
5 PUBLICATIONS **18** CITATIONS
SEE PROFILE

Weiwen Zou
Shanghai Jiao Tong University
120 PUBLICATIONS **1,111** CITATIONS
SEE PROFILE

Reduction of self-phase-modulation induced phase jitter in multiplexing repetition rate of actively mode-locked laser for photonic analog-to-digital converters

Si Chen, Guang Yang, and Weiwen Zou*
State Key Laboratory of Advanced Optical Communication Systems and Networks,
Dept. of Electronic Engineering, Shanghai Jiao Tong University,
800 Dongchuan Rd., Shanghai 200240, CHINA

ABSTRACT

We propose a novel method to multiply the pulse repetition rate of actively mode-locked fiber laser (AMLL) by spectrum-slicing and time-division-multiplexing for photonic analog-to-digital converters (PADC). Self-phase modulation (SPM) is employed to broaden the spectrum in order to obtain more parallel channels. The SPM induces additional phase jitter that degrades PADC's performance. We theoretically and experimentally show phase jitter can be effectively reduced by precise control of the tunable true-time delay array. Sampling clock of 40 GHz or higher with low phase jitter is achieved based on 10-GHz AMLL, which can be used to realize high performance PADC.

Keywords: Photonic analog-to-digital converter, actively mode-locked fiber laser, self-phase modulation, phase jitter, true-time delays

1. INTRODUCTION

Analog-to-digital converters (ADCs) transform analog signals into digital ones that can be processed easily with digital signal processor (DSP). Electronic ADC (EADC) suffers difficulty for the increasing requirements of sampling rate and precision due to electronic bottleneck. Photonic ADC (PADC) employing mode-locked fiber laser (MLL) [1,2] as sampling clock can provide favorable effective number of bits (ENOB) at ultrahigh sampling rate and is expected to have important applications in many areas such as communications, radar, medical imaging, etc. Both passively MLL (PMLL) [3,4] and actively MLL (AMLL) [5,6] have be used as the sampling clock of PADC. In contrast, the repetition rate of AMLL output pulses is around several GHz and is relatively easy to be multiplied to tens or even hundreds of GHz [5,6]. Its own time jitter has also been improved to the order of femtoseconds (fs) due to progress in microwave generator [7].

In this work, we propose a novel method to multiply the pulse repetition rate of AMLL by spectrum-slicing and time-division-multiplexing. Apart from AMLL's distinctive advantages,

*E-mail: wzou@sjtu.edu.cn; phone: +86-21-3420-5207; fax: +86-21-3420-5140

Fiber Lasers XII: Technology, Systems, and Applications, edited by L. Brandon Shaw, John Ballato,
Proc. of SPIE Vol. 9344, 93442U · © 2015 SPIE · CCC code: 0277-786X/15/$18 · doi: 10.1117/12.2077925

its bandwidth is limited (not broad enough). We employ self-phase modulation (SPM) effect to broaden the spectrum of AMLL and obtain multiple parallel channels for high speed PADC. Nevertheless, the SPM could induce additional phase jitter [8] to the broadened optical spectrum, which may degrade PADC's performance. We accurately characterize the total phase mismatches among those channels by combination of a physical model and experimental measurement. The SPM-induced phase jitter is estimated and further reduced after precisely characterizing and detuning the tunable delay line (TDL) arrays (i.e. the time-division-multiplexing), respectively. Sampling clock of 40 GHz or higher with low phase jitter is successfully achieved based on 10-GHz AMLL.

2. PRINCIPLE AND PHYSICAL MODEL

Figure 1 (a) shows the experimental configuration of AMLL based high-repetition rate sampling clock generation. The spectrum of the output waveform of AMLL has a repetition rate at 10 GHz (Calmar PSL-10-TT). It is broadened by a pulse compressor based on the effect of SPM via a pulse compressor (Calmar PCS-2) and then sliced into *M* parallel channels. We applied an optical tunable delay line (TDL) and a variable optical attenuator (VOA) to modify the time-delay and amplitude of the pulse train in each channel, respectively. Later, these pulse trains are combined together by a wavelength division multiplexer (WDM) when they are reflected by Faraday rotator mirrors laid after the TDL array. Time-wavelength mapped pulse trains at higher repetition rate are generated. In Figure 1 (b), the RF spectrum analyzer and the optical spectrum analyzer (Yokogawa AQ6370C) laid after the circulator are used to characterize the electronic and optical properties for each parallel channel or the combined pulse trains, respectively. This characterization is used for the frequency domain analysis of the amplitude and phase mismatches among the channels as referred to [6].

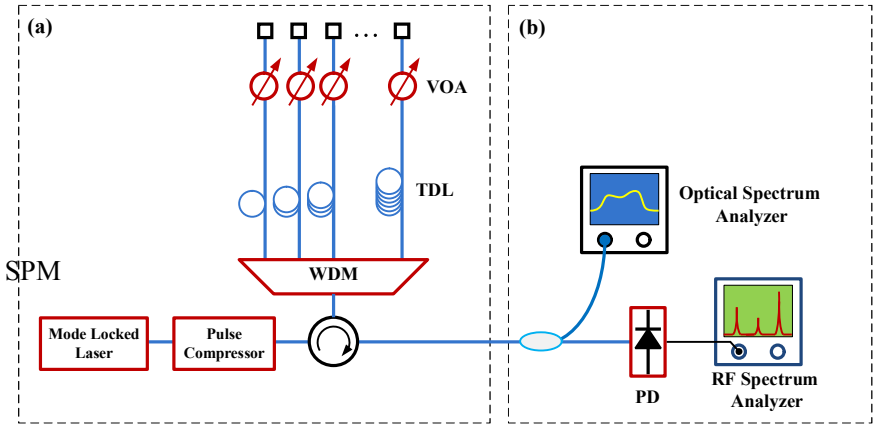

Figure 1. (a) Experimental configuration to multiply the pulse repetition rate of AMLL by spectrum-slicing and time-division-multiplexing. (b) A frequency domain measurement method. WDM: wavelength division multiplexer, TDL: tunable delay line, VOA: variable optical attenuator, PD: photon detector

For an ideal time-wavelength interleaved clock, the pulse trains in all channels are the same with no difference. That is $\tau_k = 0$, $a_k = a_0$, and $u_k(t) = u_0(t)$, where τ_k, a_k, and $u_k(t)$ is the time skew (i.e. clock timing mismatch),

amplitude, and normalized intensity temporal pulse shape in the k[th] channel, respectively. The ideal RF spectrum of the combined signal from all the channels is given by [6]

$$E(f)=\left|\frac{R_{PD}}{T_S}a_0\tilde{u}_0(f)\right|^2\sum_{m=-\infty}^{+\infty}\delta(f-mf_s), \quad (1)$$

where R_{PD} and $\tilde{u}_k(f)$ are the responsivity of the PD and the Fourier transform of $u_k(t)$, respectively. However, for the real case that τ_k, a_k, or $u_k(t)$ is not equal to zero, the RF spectrum is expressed by

$$E(f)=\left|\frac{R_{PD}}{MT_s}\sum_{k=1}^{M}a_k\tilde{u}_k(f)e^{-j2\pi f\tau_k}e^{-j2\pi(k-1)f/f_s}\right|^2\sum_{m=-\infty}^{+\infty}\delta(f-mf_s/M), \quad (2)$$

where $T_s=1/f_s$ is the sampling interval (or repetition rate) of the generated clock.

Comparing Eq. (1) and Eq. (2), noise peaks at $f=kf_s/M,(k=1,2,3,...,M-1)$ arise in the RF spectrum due to channel mismatch effects. The RF spectrum of the PADC's optical clock within the region of $[0,f_s]$ can be further describe by

$$E_k=E(kf_s/M)=\left(\frac{R_{PD}}{MT_s}\right)^2\left|\sum_{l=1}^{M}a_l\tilde{u}_l(kf_s/M)e^{-j2\pi(kf_s/M)\tau_1}e^{-j2\pi k(l-1)/M}\right|^2, k=1,2,...,M. \quad (3)$$

Define the spectrum extinction ratio η of the optical clock in the frequency domain as the ratio between the power at the fundamental harmonic of $f=f_s$ and those of the noise peaks:

$$\eta=10\log_{10}(E_s/E_n), \quad (4)$$

where E_s and E_n are given by

$$E_n=\sum_{k=1}^{M-1}E_k, E_s=E_M .$$

It is worth noting that η is an important parameter for estimating and reducing the SPM induced phase jitter (i.e. time delay) of each channel [6].

3. THEORETICAL ANALYSIS OF SPM-INDUCED PHASE JITTER

The non-linear Schrodinger equation (without dimension) [9] is:

$$\frac{\partial U}{\partial Z} = -\frac{i}{2}\left(\frac{L_0}{L_{D_2}}\right)\frac{\partial^2 U}{\partial T^2} + \frac{1}{6}\left(\frac{L_0}{L_{D_3}}\right)\frac{\partial^3 U}{\partial T^3} + i\left(\frac{L_0}{L_{NL}}\right)|U|^2 U \quad , \tag{5}$$

where $Z = z/L_0 , T = t/T_0 , L_{D_2} = T_0^2/\beta_2 , L_{D_3} = T_0^3/\beta_3 , L_{NL} = 1/\gamma P_0$, and L_0 is the length of optical fiber, T_0 is the pulse duration, and P_0 is the power of the impulse peak. The dimensionless profile of an initial input Gaussian impulse without jitter is described as

$$U(T,0) = \exp\left(-1.386T^2\right) . \tag{6}$$

Its optical spectrum can be expressed as

$$\tilde{u}(\omega) = \left|\tilde{u}(\omega)\right| e^{j\phi(\omega)} . \tag{7}$$

Because the widths of channels are relatively small in comparison with the bandwidth of optical spectrum, the phases in channels can be figured out by linear approximation:

$$\phi(\omega) = -\tau_{SPM}\omega + c.c. \tag{8}$$

Substituting $\phi(\omega)$ in Eq. (8) into Eq.(7), we get

$$\tilde{u}(\omega) = \left|\tilde{u}(\omega)\right| e^{-j\tau_{SPM}\omega} . \tag{9}$$

After the inverse Fourier Transform of Eq. (9), we get

$$F^{-1}\left[\left|\tilde{u}(\omega)\right| e^{-j\tau_{SPM}\omega}\right] = u\left(t - \tau_{SPM}\right) . \tag{10}$$

Eq. (8) shows that the physical meaning of τ_{SPM} is the time delay determining the phase jitter induced by SPM effect. The method to estimate τ_{SPM} is determined by:

$$\tau_{SPM} = -\frac{d\phi(\omega)}{d\omega} \tag{11}$$

We simulate the optical properties of AMLL before and after pulse compression and spectral splicing. The parameters are as follow: T_0=1.5ps , $L_0/L_{D_2} = -2.22\times10^{-2}$, $L_0/L_{D_3} = 1.48\times10^{-3}$, and $L_0/L_{NL} = 4.885$. The initial optical spectrum of the output of AMLL with relatively narrow bandwidth is illustrated in Figure 2(a). Figure 2 (b) shows the optical spectrum broadened by the SPM effect, providing a broadened bandwidth than Figure 2 (a). After spectral splicing, pulse trains in parallel are formed and combination in optical domain by the WDM generates the PADC's optical clock with multiplied repetition rate. Figure 2 (c) shows the optical spectrums of four channels (denoted by black lines) and their corresponding phases (denoted by dotted blue curves).

According to Eq. (11), the time delay in each channel is numerically deduced, which is summarized in Table 1. Without loss of generality, the channel 1 is always used as a reference and thus the SPM-induced time delay of other channels can be normalized with respect to the channel 1. For instance, the absolute SPM-induced time delay of the channel 1 and channel 2 are 30.55 ps and 51.36 ps while their normalized ones are 0 and 28.81 ps, respectively. It is clear that the order of the SPM induced time delays for all channels are comparable to the pulse period of AMLL (around a hundred of ps) at 10 GHz repetition rate, which theoretically indicates that SPM does affect the performance of PADC's optical clock.

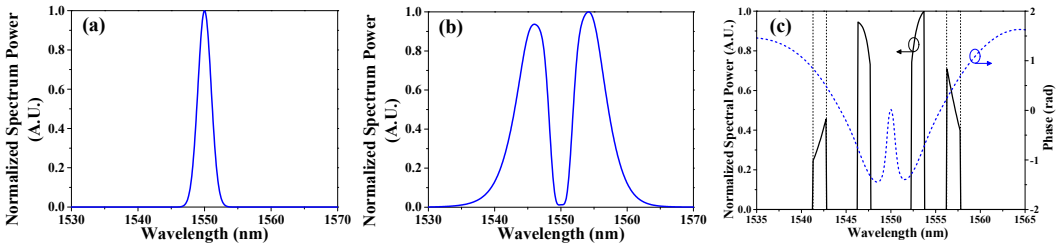

Figure 2. Simulated optical spectra of (a) AMLL, (b) pulse-compressed AMLL by SPM, and (c) the sliced output of (b). The dotted curve denotes the SPM-induced phase distribution.

Table 1. Simulated SPM-induced time delays for four channels

Channel	1	2	3	4
Normalized time delay (ps)	0	28.81	32.32	18.97

4. EXPERIMENTAL MEASUREMENT

The measured spectra of the AMLL (Calmar PSL-10-TT) with a repetition rate of 10 GHz and the compressed pulse are depicted in Figure 3 (a) and Figure 3(b), respectively. Figure 3 (c) shows the measured optical spectrum of four sliced channels after combination by a WDM. The experimental measurement matches well the simulation results (see Figure 2). In order to study the SPM-induced time delay, we first combine two channels of the channel 1 and the channel 2, 3, or 4, respectively, to produce a 20-GHz optical clock. When each combination of two channels is matched in phase and magnitude (see Eq. (3)), the inter-channel time delay should always equal to $\Delta\tau$ = 50 ps. In consequence, the RF spectrum of the combined pulses appears at the frequency of f_s = 20 GHz and the tone at the frequency of $f_s/2$ = 10 GHz (the original repetition rate of the AMLL) disappears [6]. In experiment, the time delay of the TDL array in the channel of 2, 3 or 4 is precisely adjusted while that of the channel 1 doesn't change so as to maximize the extinction ratio between the two tones at f_s = 20 GHz and $f_s/2$ = 10 GHz. Figure 4 (a) shows the RF spectrum of the combined of the channel 2 and channel 1 when they are matched. There is no other than 20-GHz tone. The similar RF spectrum of the channel 3 or 4 when combined and matched with the channel 1 is depicted in Figure 4 (b) or Figure 4(c), respectively.

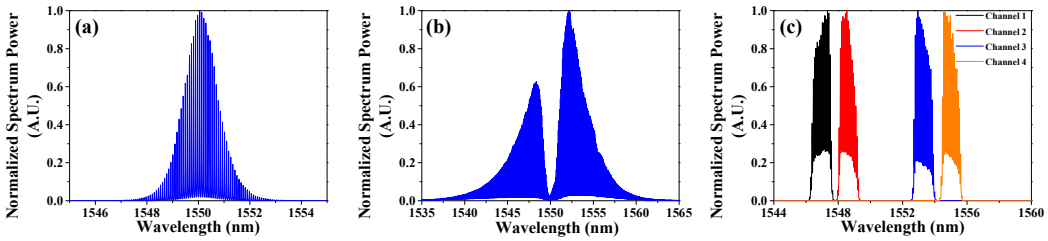

Figure 3. The measured optical spectra of (a) the AMLL at 10 GHz, (b) the SPM-compressed output, and (c) the sliced output of (b).

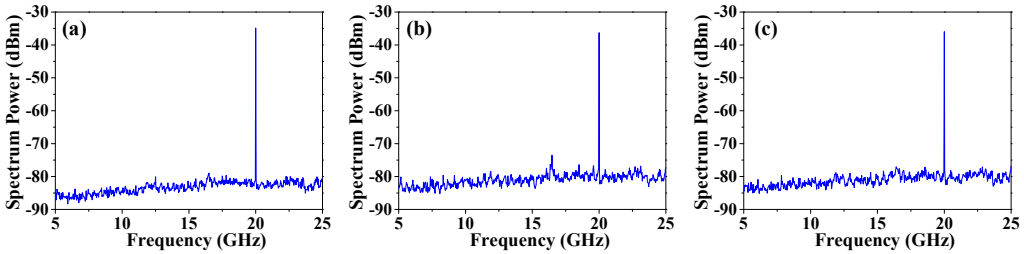

Figure 4. The RF spectrum when the channel 1 is combined with the channel 2 (a), the channel 3 (b), or the channel 4 (c). They are all matched in magnitude and phase.

In order to measure the true-time delay in each channel of the WDM-based TDL array and thus estimate the SPM-induced phase jitter (i.e. time delay), we configure the experimental setup as shown in Figure 5. First, each channel of the WDM-based TDL array depicted in Figure 5(b) is matched in phase and magnitude with the channel 1 as explained above. Second, the measurement unit (see Figure 5(a)) is used to measure the TDL array. It comprises of a tunable laser, an electro-optic intensity modulator (EOM), an optical circulator, a photo-detector (PD), and a vector network analyzer (Agilent PNAX Network analyzer N5247A). By simply detuning the wavelength of the tunable, the corresponding channel is selected. The PNA-X detects the absolute phase of each channel of the WDM-based TDL array and thus the absolute true-time delay is evaluated by the derivative of the phase on the angular frequency (see Eq. (11)). In consequence, the normalized time delay between the channel 1 and the other channel is characterized.

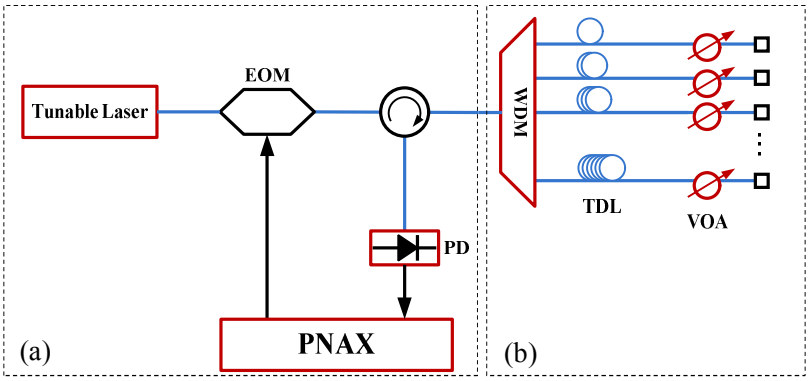

Figure 5. Experimental setup (a) to measure the absolute delay of each channel of the WDM-based TDL array (b). EOM: Electro-optic

intensity modulator, PNAX: Agilent vector network analyzer, PD: photo-detector.

Figure 6(a) illustrates the measured phase of all channels 1, 2, 3, and 4 when they are precisely adjusted for two-channel combination with the channel 1, respectively. It is clear that the absolute time delay of each channel is far away from the expected curve with the delay of $\Delta\tau$ = 50 ps, Note that the absolute time delays of all channels are quite large due to the considerable fiber length in the experimental setup (see Figure 5). They are normalized with respect to the channel 1. The measured results of the normalized time delay are different from the expected $\Delta\tau$ = 50 ps due to the existence of the SPM-induced time jitters for all channels as theoretically analyzed in Section 3. Table 2 summarizes the evaluated SPM-induced time jitters by subtracting the normalized time delay of each channel with $\Delta\tau$ = 50 ps. They are in reasonable agreements with the theoretical results given in Table 1. The variance is possibly due to the relatively rough theoretical analysis.

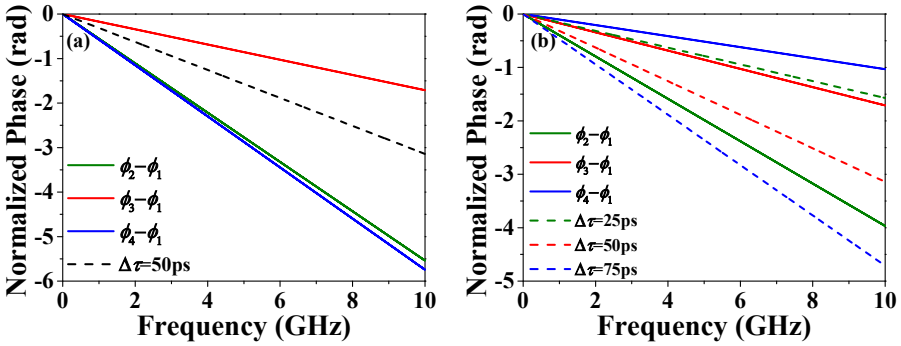

Figure 6. Measured results of the normalized phase difference between channel 2, 3, 4 and channel 1, respectively. (a) The nominal inter-channel delay is always $\Delta\tau$ = 50ps for two-channel combination. (b) The nominal inter-channel delay is $\Delta\tau$ = 25ps, 50ps, and 75ps for four-channel combination.

Table 2. Comparison of measured and evaluated time delays when two channels are combined

Channel	1	2	3	4
Nominal inter-channel delay (ps)	0	50.00	50.00	50.00
Measured absolute TDL delay (ns)	270.44661	270.53476	270.47384	270.53804
Normalized TDL delay (ps)	0	88.15	27.23	91.43
Evaluated SPM delay (ps)	0	61.85	22.77	58.57

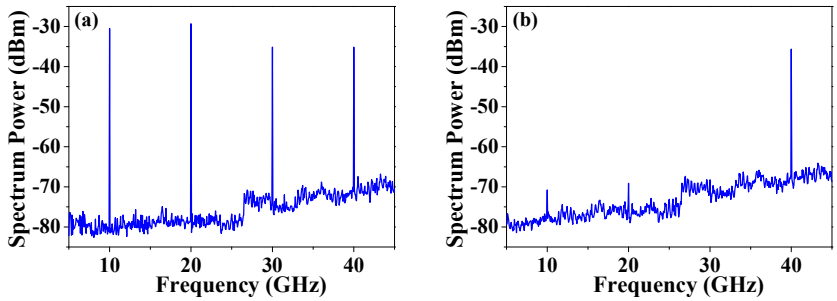

Figure 7. Comparison of the RF spectrum of four-channel combination (a) before and (b) after the compensation of SPM-induced time delay or phase jitter.

When four channels are simultaneously combined with the normalized delays of $\Delta\tau$ = 0, 25ps, 50ps, 75ps for all channels, it is expectable to achieve a PADC's optical clock with 4-time multiplexing of the AMLL's repetition rate. Figure 6 (b) shows the measured results of the normalized phases of all channels when the nominal delays are $\Delta\tau$ = 25ps, 50ps and 75ps, respectively. It is obvious that we should compensate the SPM-induced time delay so as to optimize the extinction ration defined in Eq. (4). Figure 7 compares the RF spectra of the combined channels before and after the compensation, respectively. In Figure 7 (a), the tones at 10 GHz, 20 GHz, 30 GHz and 40 GHz simultaneously exist due to the phase mismatches among channels. After compensation, only a clear tone at 40 GHz is maintained while the others disappear due to phase matches as explained in Section 2. All the adjusted and normalized delays of all channels after compensation are summarized in Table 3, providing a high precision of about 0.03 ps.

Table 3. Compensation of SPM-induced time delay for four-channel optical clock

Channel	1	2	3	4
Expected Delay (ps)	0	25.00	50.00	75.00
Adjusted absolute TDL Delay (ns)	270.44661	270.50976	270.47384	270.46304
Normalized TDL Delay (ps)	0	63.15	27.23	16.43

5. CONCLUSION

We have theoretically and experimentally studied the SPM-induced phase jitter or time delay when it is used to pulse-compress or spectrally broaden an AMLL for generation of PADC's optical clock. The experimental measurement is in a reasonable agreement with the theoretical analysis. After precise compensation of the SPM-induced time delay, a high-quality optical clock with 4-time multiplexing of the AMLL's repetition rate is successfully achieved. It is highly expectable to extend this study towards more-channel PADC's optical clock so as to achieve higher repetition rate multiplexing and higher sampling rate.

6. REFERENCES

[1]. Ober, M., Hofer, M. and Fermann, M., "42-fs pulse generation from a mode-locked fiber laser started with a moving mirror," Optics Letters 18(5), 367-369 (1993).

[2]. Li, X., Zou, W., Yang, G. and Chen, J., "Direct Generation of 148 nm and 44.6 fs Pulses in an Erbium-Doped Fiber Laser," IEEE Photonics Technology Letters 27(1), 93-96 (2015).

[3]. Li, M., Wu, G., Guo, P., Li, X. and Chen, J., "Analysis and compensation of dispersion-induced bit loss in a photonic A/D converter using time-wavelength interweaved sampling clock," Optics Express 18(20), 21162-21168 (2010).

[4]. Khilo, A., Spector, S. J., Grein, M. E., Nejadmalayeri, A. H., Holzwarth, C. W., Sander, M. Y., Dahlem, M. S., Peng, M. Y., Geis, M. W., DiLello, N. A., Yoon, J. U., Motamedi, A., Orcutt, J. S., Wang, J. P., Sorace Agaskar, C. M., Popović, M. A., Sun, J., Zhou, G., Byun, H., Chen, J., Hoyt, J. L., Smith, H. I., Ram, R. J., Perrott, M., Lyszczarz, T.

M., Ippen, E. P. and Kärtner, F. X., "Photonic ADC: overcoming the bottleneck of electronic jitter," Optics Express 20(4), 4454-4469 (2012).

[5]. Clark, T. R. and Dennis, M. L., "Toward a 100-Gsample/s photonic AD converter," IEEE Photonics Technology Letters 13(3), 236-238 (2001).

[6]. Yang, G., Zou, W., Li, X. and Chen, J., "Theoretical and experimental analysis of channel mismatch in time-wavelength interleaved optical clock based on mode-locked laser," Optics Express 2015 (in press).

[7]. Ng, W., Stephens, R., Persechini D., and Reddy K.V. , "Ultra-low jitter modelocking of Er-fibre laser at 10GHz and its application in photonic sampling for analogue-to-digital conversion," Electronic Letters 37(2), 113-114 (2001).

[8]. Wei, X., Liu, X. and Xu, C., "Numerical Simulation of the SPM Penalty in a 10-Gb/s RZ-DPSK System," IEEE Photonics Technology Letters 15(11), 1636-1638 (2003).

[9]. Agrawal, G. P., [Nonlinear Fiber Optics], Academic Press, Waltham & Massachusetts, ISBN13: 9780123970237 (2012).